Drug Development and Industrial Pharmacy, 2012; Early Online: 1–11

ISSN 0363-9045 print/ISSN 1520-5762 online
DOI: 10.3109/03639045.2012.679361

informa
healthcare

RESEARCH ARTICLE

A simple method of microneedle array fabrication for transdermal drug delivery

Jaspreet Singh Kochhar, Wei Jiang Goh, Sui Yung Chan, and Lifeng Kang

Department of Pharmacy, National University of Singapore, Singapore

Abstract

The outermost layer of skin, stratum corneum, being lipophilic limits the passive transport of hydrophilic and large molecular weight drugs. Microfabrication technology has been adapted to fabricate micron scale needles, which are minimally invasive, yet able to deliver the drugs across this barrier layer. In this study, we fabricated microneedles from a biocompatible polymer, namely, poly (ethylene glycol) diacrylate. A simple lithographical approach was developed for microneedle array fabrication. Several factors including polymerization time, ultraviolet light intensity and distance from light source were studied for their effects on microneedle formation. The microneedle length and tip diameter can be controlled by varying these factors. The microneedles were shown to be able to penetrate cadaver pig skin. Model drug rhodamine B was encapsulated in the range of 50 μg to 450 μg per microneedle array. The fabricated microneedles containing rhodamine B increased the permeability by four times than the control. Altogether, we demonstrated that the microneedle arrays can be fabricated through a simple single-step process and needles were mechanically strong to penetrate skin, increasing the permeability of encapsulated drug through skin.

Keywords: Microneedles, photolithography, transdermal drug delivery, polymer

Introduction

Transdermal delivery systems include topical formulations and more recently, transdermal patches. The outermost layer of epidermis, stratum corneum, prevents molecules larger than 500 Da from passively diffusing to the subcutaneous tissues[1]. The macromolecules cannot cross the stratum corneum at therapeutically useful rates. Therefore, creating delivery systems to deliver these big molecules has been a major challenge for formulation scientists in the past decade.

To deliver these big molecules, an array of methods have been researched, including chemical penetration enhancers[2], iontophoresis, ultrasound[3], laser[4] and electroporation[5]. The high precision microelectronic tools and miniaturization techniques, first adapted in the semiconductor industry, have been tailored to design micron scale drug delivery systems. Microneedles which are small micron scale projections varying in height and shape are an example of such an innovation. They are applied to the skin in a manner similar to transdermal patches to create pores, allowing the passage of hydrophilic drugs, mimicking the action of hypodermic needles. They can therefore be considered a hybrid of the safe and convenient transdermal patch and efficient hypodermic injections.

Since microneedles are in the micron scale in length, they do not penetrate deep into the skin to stimulate the nerves and are relatively pain-free[6]. The pores created by microneedles have been shown to close within 72 h after removal of the microneedles[7]. This makes the use of microneedles very appealing to patients with impaired healing and those requiring frequent injections (e.g. diabetic patients). Lastly, microneedles are amenable to self administration. The drug moiety could either be coated on the microneedles or encapsulated in the core or the skin can be pre treated with microneedles followed by conventional application of gel or patch.

Address for Correspondence: Lifeng Kang, Department of Pharmacy, National University of Singapore, 18 Science Drive 4, 117543, Singapore. Tel.: +65 6516 7519; Fax: +65 6779 1554. E-mail: lkang@nus.edu.sg

(Received 12 January 2012; revised 06 March 2012; accepted 14 March 2012)

Microneedles have been fabricated from silicon[8,9], metals[10–13], zeolite[14] and polymers[15–20]. Extensive and complicated multi-step processes, requirement of clean room facilities and biocompatibility are potential hindrances of using silicon as a material for biomedical use. Some metals have been approved by FDA for biomedical applications and are used for microneedle fabrication. They are robust but pose the potential risks of infection on reuse, breaking off in the skin and generate biohazardous sharps. These challenges have led the search for more viable substitutes to fabricate microneedles.

Polymeric microneedles have received attention recently with several fabrication methods being developed. Polymers including poly (vinyl pyrrolidone)[15], its co-polymer with methacrylic acid[15] and poly-lactide-co-glycolide[21] have been used. Sugars and sugar derivatives like dextrose[17], maltose[22], galactose[23], carboxymethylcellulose[16] and amylopectin[16] have also been reported for fabricating microneedles. These materials were found to be biocompatible, cost-effective and generate no biohazardous waste.

Despite some special advantages over their silicon and metallic predecessors, microneedles fabricated from polymers and sugars present some processing concerns. Microneedles developed from sugars[18,24] pose processing difficulties due to high melting points of sugars (140–160°C) and substantial losses in the drug content have been observed[24]. Similarly, high temperatures have been used for the casting methods used by other groups for fabricating polymeric microneedles[16,21]. A microneedle roller device recently developed by their group also involves the use of elevated temperatures[25]. Fabrication from other sugars such as dextrin using a thread forming process with polypropylene[7,17] or polyethylene tips[26], has been adapted for single-needle/micropile fabrication, which may limit the amount of drug encapsulation[27]. Other methods involve techniques such as deep X-ray lithography, ultraviolet lithography, wet silicon etching and reactive ion etching, lens based lithographic patterning, photopolymerization with longer exposure to UV light and laser based fabrication involve sophisticated equipments which accrue the overall cost of the process and make it potentially inaccessible to many researchers.

In this study, we develop a simple photo-polymerization method to fabricate microneedles with poly (ethylene glycol) diacrylate (PEGDA) owing to its known biocompatibility[28] and FDA approval for human use[29]. It has a long history as non toxic and non immunogenic polymer, widely used for several drug delivery applications[30]. Compared with the photo-crosslinkable monomer vinyl pyrrolidone[15,31], the macromer PEGDA can be cross-linked in short time under UV (a few seconds). In addition, PEGDA used in this study (Mn = 258) has a larger molecular weight than vinyl pyrrolidone (MW = 111), which may indicate better biocompatibility[32]. Moreover, its extensive use as a substrate for tissue engineering[33,34] also makes it a potentially useful biomaterial for microneedle fabrication. The fabrication method is based on photolithography, involving exposure of the polymer to UV light through a patterned mask in a single step process. The method offers the advantage of short exposure to UV light. It is similar to the commercial manufacture of contact lenses, which also employs a mask based photolithography method to polymerize the monomers[35], suggesting that our process lends itself suitable to be scaled up commercially for industrial applications.

Materials and methods

Materials

PEGDA (Mn = 258), 2-hydroxy-2-methyl-propiophenone, (HMP), 3-(trimethoxysilyl) propyl methacrylate (TMSPMA) and trypan blue solution (0.4%) were purchased from Sigma-Aldrich (St. Louis, MO). Rhodamine B was purchased from Alfa Aesar (Lancaster, UK). All materials used were reagent grade and were used as received. Water purified using Millipore Direct-Q® (Molsheim, France) was used in the studies.

Coating of glass coverslips

Glass coverslips (Menzel Glaser, Germany, 190 micron thickness, 22 × 22 mm) were first rinsed with 70% ethanol and air dried. Later, they were immersed in 0.4% TMSPMA solution overnight for coating. The coverslips were then washed with water and baked for 2 h at 70°C. TMSPMA molecules attach to the silanol groups on the glass. The resultant chemical interaction is depicted in Figure 1.

Fabrication of microneedle backing layer

Two uncoated coverslips were supported on either side of a glass slide (Sail Brand, China) as 'spacers' as shown in Figure 1A. A TMSPMA coated coverslip was placed on this setup to create a cavity in the centre, approximately 190 μm thick. PEGDA, containing 0.5% w/w HMP (referred as the prepolymer solution) was wicked by capillary action into the cavity. The set up was then irradiated with high intensity ultraviolet light (11.0 W/cm^2) for 1.5 sec using UV curing station with a UV filter range of 320–500 nm (OmniCure® S200-XL, EXFO Photonic Solutions Inc., Canada). The intensity of the UV light was measured with the OmniCure® R2000 radiometer. A collimating adaptor (EXFO 810-00042) was used with the UV light probe. TMSPMA molecules bonded to the glass coverslips are covalently linked to the acrylate groups of PEGDA via free-radical polymerization[36,37] (Figure 1, within dashed ellipses). The backing layer approximately 190 μm thick was then easily removed from the setup.

Fabrication of microneedles

The set up for fabrication of microneedles is similar to that for microneedle backing except for number of 'spacers'. Increased spacer thickness was achieved by increasing the number of coverslips stacked on either side of the glass slide as shown in Figure 1B. The prepolymer solution was

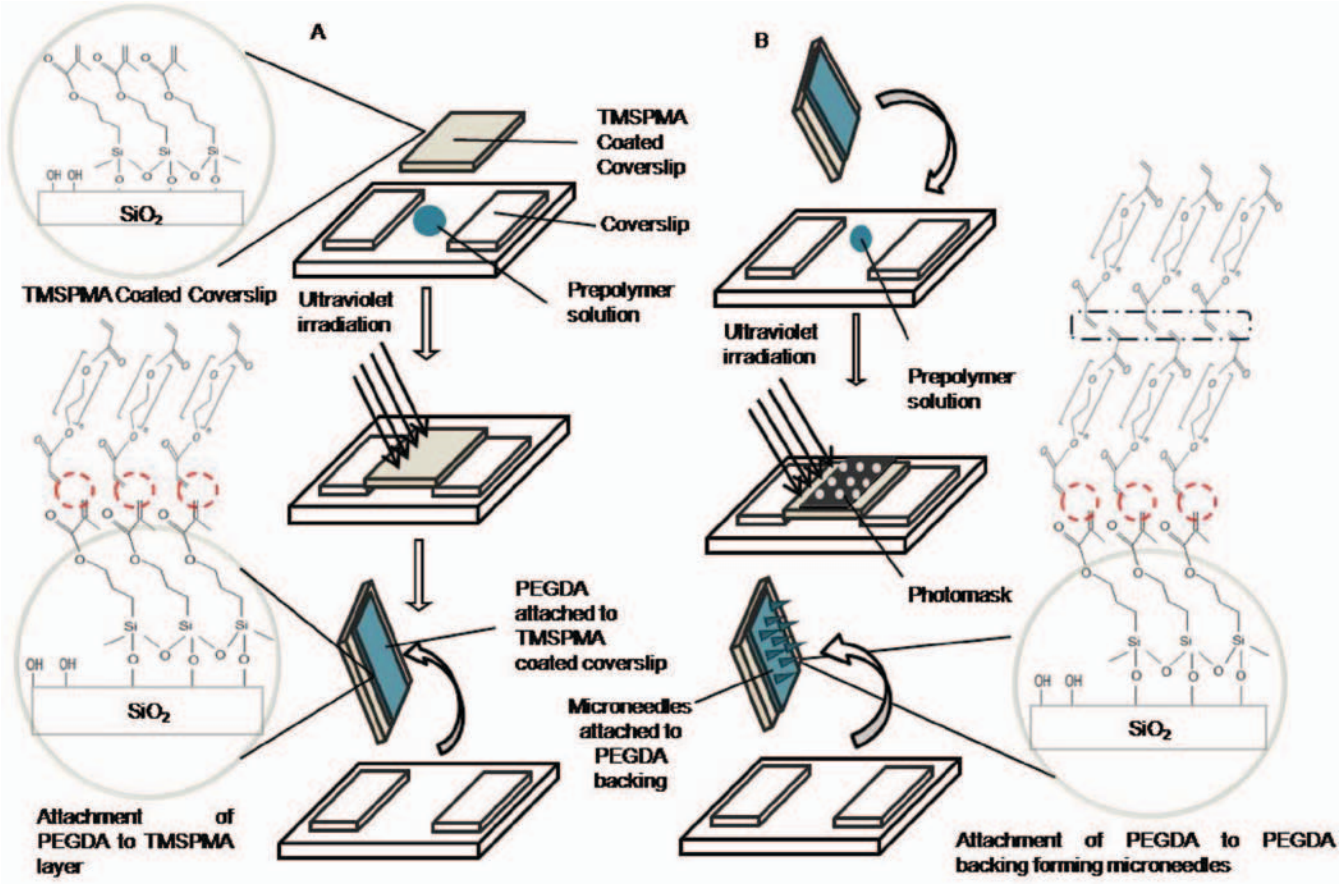

Figure 1. (A) Schematic representation of the fabrication process. PEGDA is attached to TMSPMA coated coverslip via free radical polymerisation using UV irradiation, forming the backing for microneedles. (B) Using glass slides as support, the PEGDA backing is mounted onto the set-up with PEDGA filled in the enclosed cavity. Subsequently, the set-up is irradiated with UV light. UV light is only able to pass through the clear regions on the photomask, forming microneedles.

then similarly wicked by capillary action into the cavity. A plastic film (called as *photomask*) was inked specifically in the pattern of microneedle array. The background of this film was inked leaving small circles in an array pattern transparent to allow the UV light to pass through. The transparent circles govern the base diameter of the microneedles. Similarly, the center-to-center spacing between two microneedles can be controlled. Such a film was placed on the coverslip carrying the microneedle backing and the setup was irradiated with UV light. The use of photomask blocked the UV access in the inked regions and allowed the UV light to pass through the transparent circles, which resulted in the formation of microneedles. The microneedles were covalently bonded with the PEGDA macromers in the backing layer to form an interpenetrating polymer network[36,37] (Figure 1B, within dashed rectangles). The microneedle structures, attached to the coverslip, were carefully removed from the glass slide and washed with water to remove the uncross-linked prepolymer solution. The prepared microneedles were imaged using Nikon SMZ 1500 stereomicroscope (Nikon, Japan), to quantify the microneedle geometric characteristics.

Microneedle insertion in pig skin

Ascertaining that microneedles penetrate the skin, PEGDA microneedles, in an 8 × 8 array were inserted into excised cadaver pig skin obtained (after the pig was sacrificed using CO_2 asphyxiation) from a local abattoir. The hair was first removed using an electric hair clipper (Philips, Hong Kong) followed by hair removal cream *Veet* (Reckitt Benckiser, Poland) to completely remove the hair[38]. The skin samples were cleaned and stored at –80°C until use. Prior to use, the subcutaneous fat was removed using a scalpel. The skin was fixed fully stretched on a thin (7-8 mm) layer of modelling clay (Nikki, Malaysia), to mimic the tissue-like mechanical support. Microneedles were inserted using the force of a thumb on the backing layer for approximately 1 min.

The arrays were then removed and the area of insertion was stained with trypan blue for 5 min, which specifically stains the perforated stratum corneum sites. The excess stain was washed away with water. The areas stained with the dye were viewed by brightfield microscopy using Eikona Image Soft Microscope (China). A positive control, which consisted of a 27 gauge hypodermic needle, was used to create perforations in the form of a 4 × 3 array. Intact skin stained with trypan blue was used as a negative control.

Histological examination of the skin was also carried out by the microneedle-treated skin samples in to 10 μm sections using a microcryostat (Leica, Germany). The histological sections were stained with hematoxylin and eosin and imaged by stereomicroscopy. All animal experiments were approved by Institutional Animal Care and Use Committee (IACUC), National University of Singapore (NUS).

Encapsulation of a model drug: imaging and *in vitro* release

Rhodamine B was dissolved in the prepolymer solution at a concentration of 0.09, 0.17 and 0.44 weight %, respectively. The drug-laden microneedle samples were imaged using a fluorescence stereomicroscope SMZ - 1500 (Nikon). The amount of drug encapsulated in the microneedles was calculated from the percent weight of the drugs in the prepolymer solution and the weight of fabricated microneedles. Selective incorporation of rhodamine B in the backing layer or microneedle shafts was made possible by using the prepolymer solutions containing the model drug to fabricate the backing layer or microneedles respectively. *In vitro* release of rhodamine B was tested by suspending fabricated microneedle arrays in 15 ml of 1 × PBS, at 37°C and sampled at regular intervals. At each sampling point, the whole 15 ml of release medium was withdrawn and replaced with 15 ml of fresh 1 × PBS. The samples were stored at 4°C before analysis. The amount released was quantified by measuring rhodamine B fluorescence at excitation and emission wavelengths of 554 nm and 586 nm, respectively, with a Tecan 2000 microplate reader (Tecan, Switzerland)[39].

In vitro permeation through rat skin

To analyze the increase in skin permeability following microneedle application, cadaver rat skin was used. The subcutaneous fat was removed with a scalpel. Microneedles containing 50 μg of rhodamine B were applied to the skin samples. As a comparative control, a similar concentration of rhodamine B in propylene glycol solution in the donor compartment was used. Skin was mounted on a side-by-side diffusion cell (TK-6H1, Shanghai Kai Kai Science and Technology Co., Ltd, China) with receptor compartment containing 4.5 ml of 1 × PBS with 0.005% v/v sodium azide (Alfa Aesar). For each group, six replicates were used. Water was circulated at 37°C and the donor and receptor solutions were continuously stirred at 250 rpm with magnetic stirrers. The samples were collected at regular intervals over a period of 48 hours. At each sampling point, 1 ml of receptor medium was withdrawn and replaced with 1 ml of fresh PBS. The samples were stored at 4°C before analysis. All the sample vials were centrifuged at 10,000 rpm and supernatant was analyzed by measuring rhodamine B fluorescence as previously mentioned. Cumulative amount of drug permeated against time and skin permeability was calculated by assuming steady state flux.

Statistical analysis

Testing of microneedle geometric properties, eight microneedle arrays were fabricated for each parameter studied and mean ± standard deviation was reported. For other experiments, results from triplicate or more measurements were used to compute mean and standard deviation. One-way ANOVA was used, for analyzing multiple groups of data or statistical differences. Results with p value of less than 0.05 were considered to be statistically significant.

Results

Fabrication of polymeric microneedles

Effect of varying UV light parameters

Microneedles were fabricated to ascertain the effect of various variables such as polymerization time, UV light intensity and distance from UV light source on microneedle length and tip diameter. All microneedles fabricated had a base diameter of 300 μm and center-to-centre spacing of 1500 μm. The spacer thickness between the base glass slide and the TMSPMA coated coverslip (with the microneedle backing layer attached to it) was kept constant at 1330 μm. All microneedles were viewed and the dimensions were measured by using a Nikon SMZ 1500 stereomicroscope.

Effect of varying polymerization time

Microneedles were fabricated at different polymerization times ranging from 0.5 to 4 sec, keeping the UV light intensity (11.0 W/cm^2) and the distance from UV light source (3.5 cm) constant. Uniform microneedle arrays cannot form at times below 1 sec (supplementary Figure SA). At polymerization times beyond 1 sec microneedles started to form with an average length of 1218 ± 18 μm until the exposure time of 2 sec ($p > 0.05$). Beyond that, the microneedle length increased to an average of 1268 ± 16 μm till a maximum exposure time of 4 sec ($p > 0.05$) (Figure 2A). Similarly, for times up to 2 sec, the tip diameter averaged 131 ± 18 μm, which increased to 163 ± 17 μm with increase in exposure time between 2.5 and 4 sec (Figure 2B). Higher polymerization times may have resulted in higher microneedle strength which is important for microneedle penetration in skin.

Effect of intensity of UV light

The intensity was varied between 1.15 and 11.0 W/cm^2 maintaining the polymerization time (3.5 sec) and distance from UV light source (3.5 cm) constant. Uniform microneedle arrays cannot form below the strength of 2.21 W/cm^2 (supplementary Figure SB). Microneedle length averaged at 1250 ± 4 μm and varying the intensity had insignificant effect on the microneedle length ($p > 0.05$) (Figure 2C). Average tip diameter of microneedle tip was found to be 154 ± 8 μm ($p > 0.05$) (Figure 2D). The microneedles fabricated at 11.0 W/cm^2 were observed to

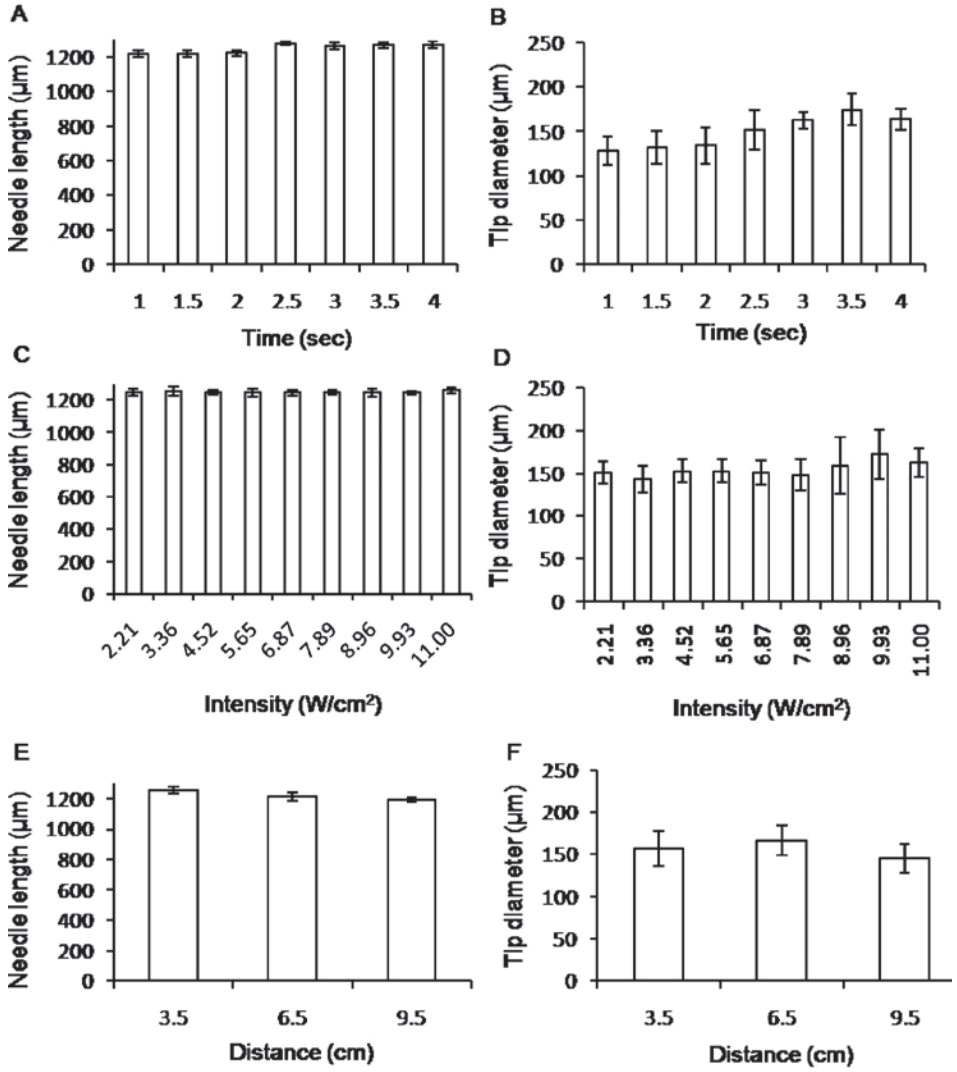

Figure 2. Effect of UV parameters on microneedle geometry. Effect of (A) polymerization time, (C) intensity and (E) distance from UV source on microneedle length. Effect of (B) polymerization time (D) intensity and (F) distance from UV source on tip diameter.

be strong enough to be used for subsequent penetration experiments.

Effect of varying distance from UV light source

Variation of intensity of UV light with increase in the distance from the light source was tested for its influence on the microneedle length and tip diameter. For this purpose, the fabrication stage was placed at a distance ranging, 3.5–9.5 cm from the light source. Microneedles were fabricated at several distances within this range, keeping other variables of polymerization time (3.5 sec) and ultraviolet light intensity (11.0 W/cm^2) constant. It was observed that as the distance was increased, the microneedle length decreased from 1256 ± 21 µm to 1190 ± 70 µm. However the difference was found to be statistically insignificant between the distances 3.5–6.5 cm and 3.5–9.5 cm (Figure 2E). Increasing the distance of the fabrication stage beyond 9.5 cm resulted in the formation of non uniform arrays of microneedles with variable lengths (supplementary Figure SC). Tip diameter averaged at 156 ± 10 µm with the increase in distance from 3.5 cm to 9.5 cm (Figure 2F).

Effect of non UV light parameters

Effect of spacer distance

For targeting the drugs to specific areas of the skin, it is essential to have a definite control over the microneedle length. We manipulated the spacer thickness by increasing the number of coverslips stacked on the base glass slide (Figure 1). Such a successive increase in the space between the base glass slide and the TMSPMA coated coverslip (which has PEGDA backing fabricated on it), increases the microneedle length (Figure 3A–3F). At each step one coverslip was added to the stack and thus increasing the spacer thickness by approximately 190 µm. The spacer thickness could be varied between 380 and 1330 µm. The UV parameters were kept constant at UV intensity (11.0 W/cm^2), polymerization time (3.5 sec) and distance from UV source (3.5 cm). In this manner, the microneedle length could be varied between 299 ± 8

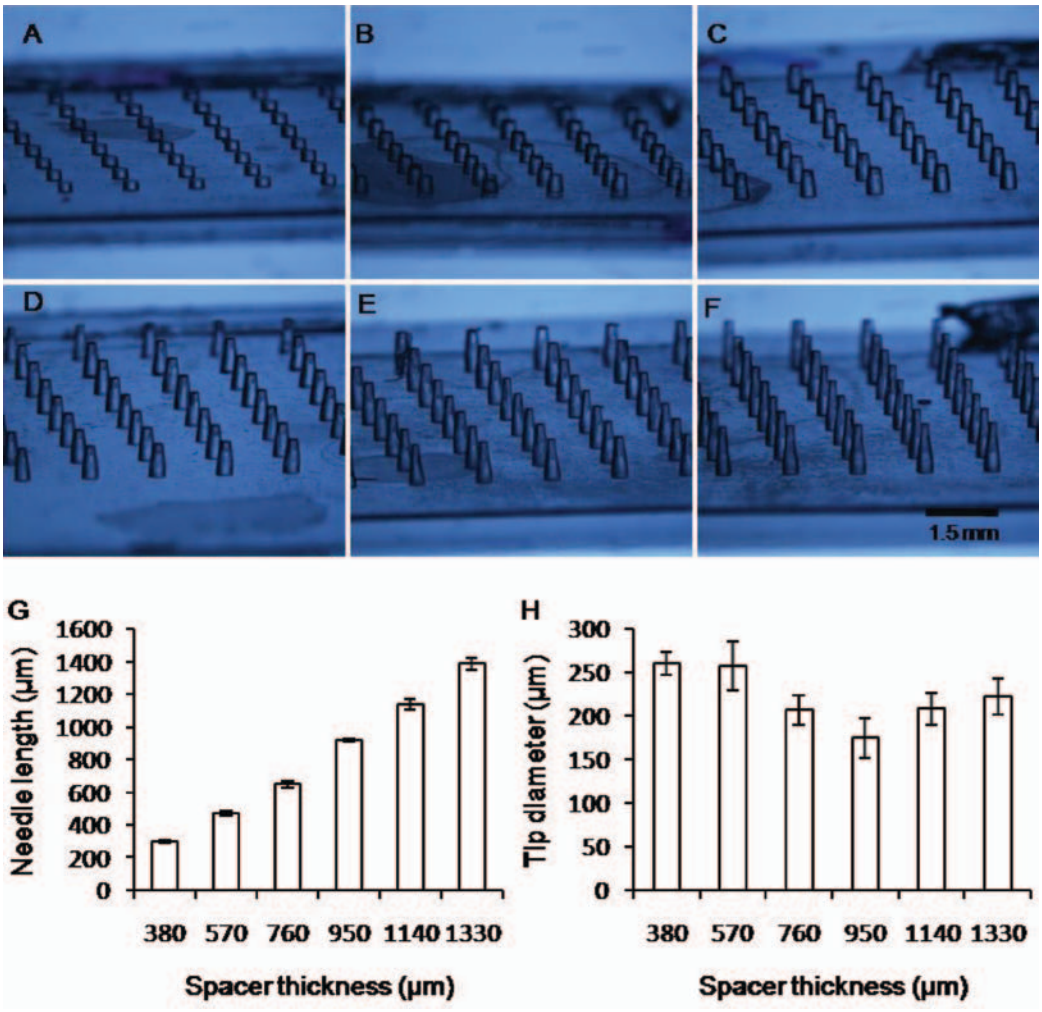

Figure 3. Effect of increasing spacer thickness. (A–F) Images at various spacer thickness, with microneedle length of 252, 441, 680, 820, 1044 and 1211 µm, respectively. (G) Increase in microneedle length with increase in spacer thickness. (H) Decrease in the tip diameter with increase in spacer thickness.

µm and 1387 ± 35 µm (ANOVA, $p < 0.001$) which is corroborated by the average coverslip thickness of 190 µm each (Figure 3G). An increase in the spacer thickness also resulted in a corresponding decrease in the tip diameter of the microneedles. The tip diameter ranged from 174 ± 22 µm to 260 ± 13 µm (Figure 3H).

Microneedle penetration in pig skin

Microneedles measuring 921 ± 31 µm in length were inserted in cadaver pig skin. Penetration of microneedle arrays in the skin was demonstrated using the trypan blue staining method. Figure 4A shows the image of a microneedle array penetration after staining. The blue spots are specifically stained at the points of microneedle insertion. Penetration with a hypodermic needle as a positive control and staining with trypan blue to ascertain the staining specificity and capability of the dye is displayed in Figure 4B. As a negative control, the dye was applied on intact skin. After washing, the stain was removed, proving that the blue dye only stains the sites of stratum corneum perforation (Figure 4C). The microneedles were not deformed upon removal from the skin suggesting that they were robust enough to penetrate the skin. Figure 4D shows the histological section prepared after microneedles were inserted and removed subsequently. Hematoxylin and eosin staining to visualize the skin layers displays a clear indentation left by microneedle penetration. The microneedle penetrated almost completely into the skin suggesting that the encapsulated drug can be delivered efficiently.

Encapsulation and *in vitro* release of encapsulated model drug

Figure 5A shows the microneedles fabricated from PEGDA, in which no model drug has been incorporated. As observed from Figure 5B, the microneedle shafts contain the red colored rhodamine B, whereas there is no fluorescence observed from the backing layer. Conversely, in Figure 5C, the microneedle shafts do not contain any

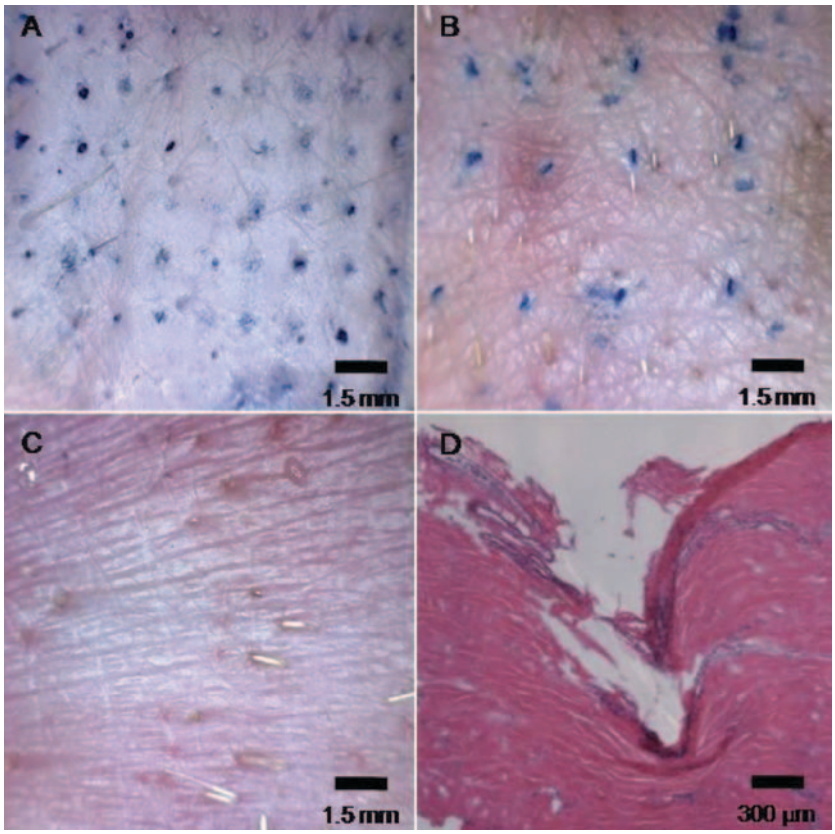

Figure 4. Penetration of microneedles in cadaver pig skin. (A) Area of microneedle penetration stained with trypan blue. (B) A positive control with skin penetrated using a 27 gauge hypodermic needle (4 × 3 array) and holes stained by trypan blue. (C) Negative control (no microneedles) applied on the skin, subsequently stained by trypan blue. (D) Histological section of skin stained with hematoxylin and eosin post microneedle application.

rhodamine B dye and the fluorescence is only observed in the backing layer, which specifically contains the dye. The drug can also be incorporated in both microneedles as well as the backing, which were also fabricated during this study (Figure 5D).

The release of encapsulated rhodamine B was studied over a period of 1 week. It was observed that nearly 30% of the encapsulated drug was released within the first hour (Figure 6A). The drug release continued as the drug loaded in the backing layer potentially serves as a reservoir. The percentage amount released was independent of the concentration of the drug in the microneedles and the backing layer. The actual amount released was shown in Figure 6B.

In vitro permeation through rat skin

The ability of microneedles to increase skin permeability of rhodamine B was assessed. Microneedle increased the total amount permeated by 3.89-fold as compared to a propylene glycol solution of rhodamine B (Figure 7). The steady-state flux was 0.299 ± 0.1 µg/cm^2/h for microneedle and 0.067 ± 0.01 µg/cm^2/h for propylene glycol solution, which is 4.35 times lower ($p < 0.05$).

Discussion

Many groups have successfully developed polymeric microneedles using various techniques and polymeric materials[7,16,17,21,26]. Previous studies to develop polymeric microneedle arrays have used multi-step methods involving development of master structures to create reverse molds[16], use of vacuum to fill the molds with the polymer substrate, longer exposure to UV radiation to polymerize the base substrate[15] and use of high temperature micro-molding techniques[24]. The processing conditions used in these methods may have an adverse effect on drug molecules, such as peptides and proteins.

We developed a one-step lithographical method to fabricate microneedles. The major equipment in this method is the UV curing station[33]. The fabrication process involved free radical polymerization using the photoinitiator HMP, which initiates the polymerization reaction in the presence of UV. Polymerization time ranging from 1 to 4 sec is not expected to compromise the stability of encapsulated drugs. The fabrication set up does not have specific requirements of vacuum or heating arrangements.

Fabrication of microneedles from PEGDA began with the process of optimization of fabrication conditions. As

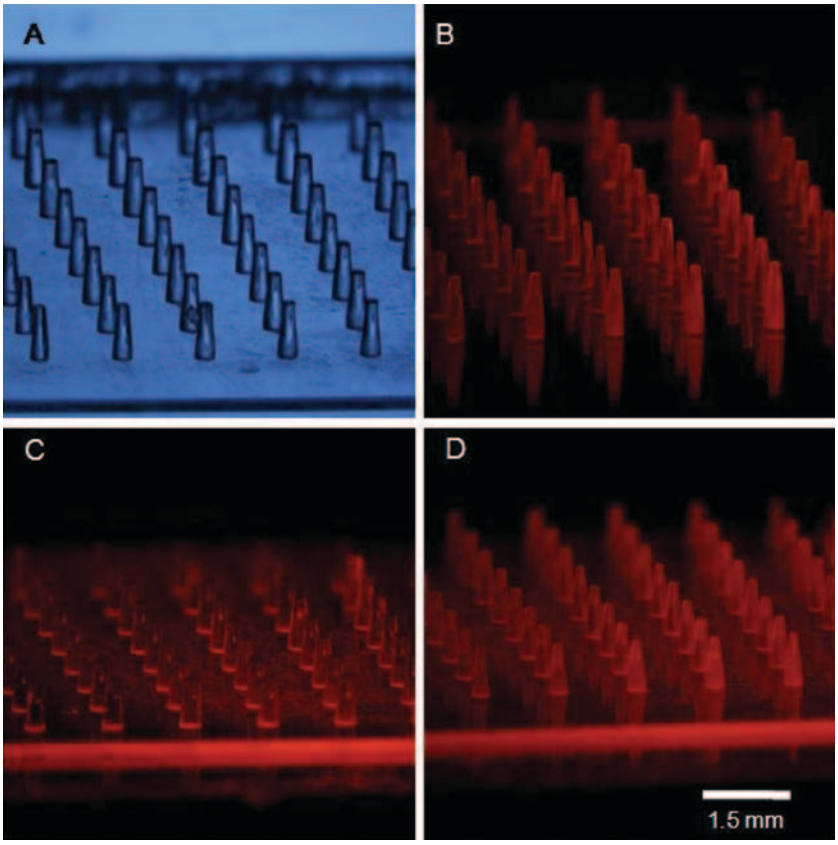

Figure 5. Incorporation of rhodamine B in microneedle arrays. (A) Without rhodamine B, (B) rhodamine B in microneedle shafts, (C) rhodamine B in backing layer and (D) rhodamine B in both microneedle shafts and backing.

we were developing this method to fabricate microneedles using ultraviolet light governed photo polymerization, several variables were studied. The polymerization time (time of exposure of polymer to ultraviolet light), ultraviolet light's intensity and the distance of the fabrication assembly from the ultraviolet light source was considered as factors influencing microneedle fabrication and were evaluated for their effect on microneedle geometry.

The time of exposure to UV light, defined as the polymerization time, is important with respect to the microneedle geometric properties as well the encapsulated drug stability. Ultraviolet light has been well known to cause primary photooxidation, which is the major contributor to drug degradation[40]. One of the aims of our experiments was to study the geometric properties and develop a method of fabricating microneedles in the shortest possible polymerization time. The photopolymerization methods used to date involved long exposure times to UV in the range of 30 min[15]. With the new approach, microneedle structures were obtained at low polymerization time of 1–4 sec. Although microstructures could be formed at lower polymerization times as well, but as the time was increased the microneedle strength increased. A polymerization time of 3.5 sec was used for microneedles fabricated in the current study as it resulted in robust microneedle arrays enabling penetration in skin. On the other hand, photopolymeric reactions can also be influenced by the intensity of the light source used[41]. We aimed to find the right combination of polymerization time and the UV intensity for fabricating robust microneedles. It was found that a combination of polymerization time of 3.5 sec and intensity of 11.0 W/cm^2 was suitable for our method.

Penetration of microneedles in cadaver pig skin revealed that microneedles penetrated the skin using a thumb with little force. Trypan blue is a hydrophobic dye and is known to specifically stain the sites of stratum corneum perforation, which is confirmed by histological sectioning of the skin. Microneedles are intended to create transient pores in the skin structure and release the drug through these pores. These pores have been previously shown to close within 72 h upon microneedle removal[7] and microneedle application has been associated with a lower risk of microbial infection as compared to hypodermic needles[42].

Polymeric microneedles offer the advantage of incorporating the drugs in the polymeric matrix as compared to silicon or metallic counterparts where the drug can only be coated on pre-fabricated microneedles. Incorporation of drugs in microneedles fabricated from PEGDA demonstrates the encapsulation efficiency of PEGDA microneedles. The drugs have been incorporated either in the microneedle shafts for bolus release or in the backing layer for sustained release or in both

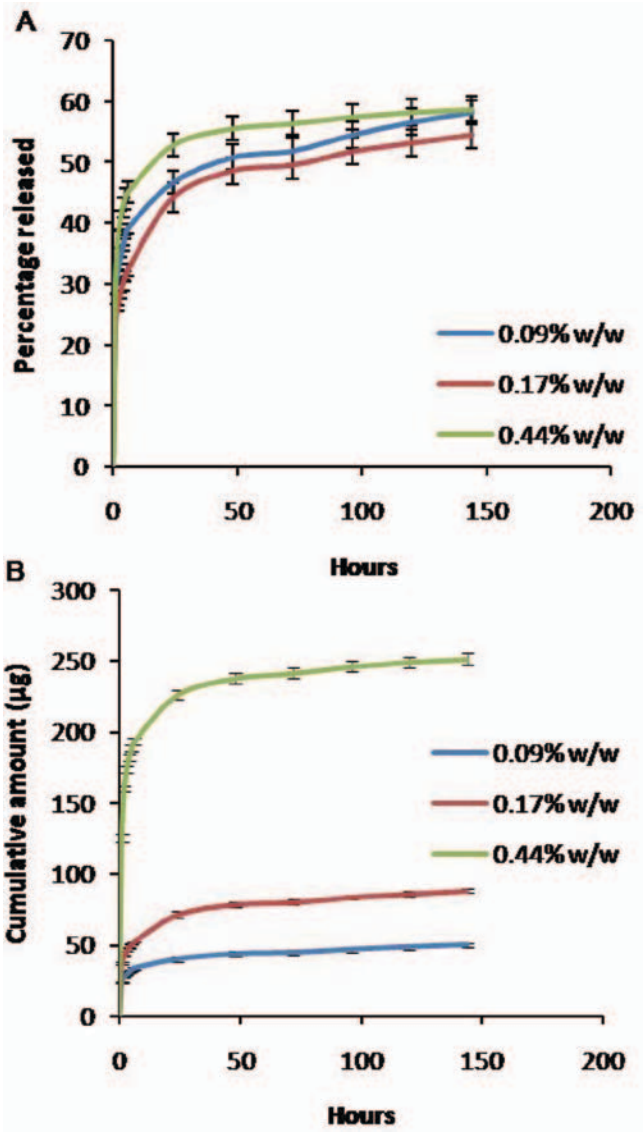

Figure 6. Release profile of rhodamine B encapsulated in microneedles over a period of 1 week. (A) percentage released (B) cumulative amount released.

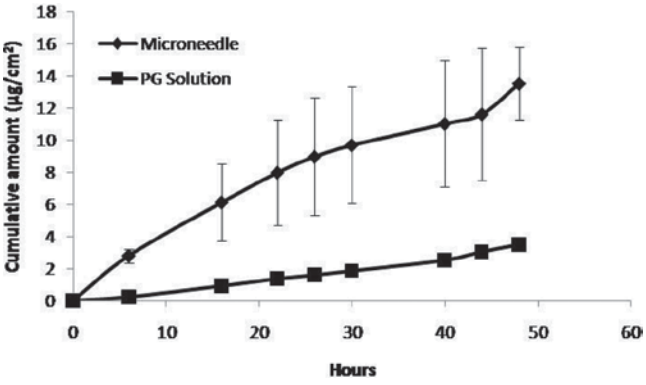

Figure 7. Cumulative amount of rhodamine B permeated through rat skin when microneedle patch and propylene glycol solution of rhodamine B were applied over a period of 48 h.

layers for a prolonged effect[16]. The drug release from the microneedles in the surrounding subcutaneous tissue is followed by release of the drug encapsulated in the backing layer, which continues to release the drug through the transient pores created by the microneedles. Since it is possible to incorporate a larger amount of drug in the backing layer as compared to the microneedles, it is useful to incorporate the drug both in the microneedles and the backing layer to increase drug loading. The drug encapsulated was released with a burst upfront in the first hour, which was followed by slower release over a period of 1 week of the study. This can be attributed to the reservoir capacity of the backing layer which can release the drugs through the microneedles inserted into the skin. The drug release properties, however, may be modified by coating the microneedles or incorporating varying amounts of release modifying polymers, such as chitosan, to control the release of the drug from the PEGDA matrix. Chitosan as a coating material for controlling the release rates has been previously investigated[43]. Other photo-crosslinkable polymers may also be used to alter the release profile of the drugs.

Drug laden microneedles created transient pores which may have led to a higher flux as compared to a control, which included a propylene glycol solution containing the same amount of the drug as in one microneedle array. The microneedles increased the flux by over four times compared to passive diffusion of rhodamine B through the capillary intercellular pathways in the stratum corneum, which was the main mode of drug transport across the skin for a propylene glycol solution[44].

Conclusion

We developed a simple photolithographical approach to fabricate polymeric microneedles. Microneedles were found to be capable of penetrating cadaver pig skin when inserted with the force of a thumb. A model drug, rhodamine B could be encapsulated in the polymeric matrix of the microneedle shafts and the backing layer and released in an *in vitro* release medium. The microneedles, when applied to rat skin, increased the flux of encapsulated rhodamine B by 4 times over passive diffusion of a solution. The approach is amenable to other photo cross linkable polymers and potentially useful for transdermal drug delivery. Moreover, the method may be potentially scaled up for mass production of microneedle arrays.

Acknowledgements

We thank Ms. Joleen Lim of SBIC-Nikon Imaging Centre, Singapore for the assistance provided in imaging the microneedle samples. J.S.K. is a recipient of NUS research scholarship.

Declaration of interest

This work was supported by a startup grant from National University of Singapore. The authors report no conflict of interest and are solely responsible for the content of this manuscript.

References

1. Bos JD, Meinardi MM. (2000). The 500 Dalton rule for the skin penetration of chemical compounds and drugs. Exp Dermatol, 9:165–169.
2. Kang L, Yap CW, Lim PF, Chen YZ, Ho PC, Chan YW et al. (2007). Formulation development of transdermal dosage forms: quantitative structure-activity relationship model for predicting activities of terpenes that enhance drug penetration through human skin. J Control Release, 120:211–219.
3. Lee SE, Choi KJ, Menon GK, Kim HJ, Choi EH, Ahn SK et al. (2010). Penetration pathways induced by low-frequency sonophoresis with physical and chemical enhancers: iron oxide nanoparticles versus lanthanum nitrates. J Invest Dermatol, 130:1063–1072.
4. Lee WR, Shen SC, Wang KH, Hu CH, Fang JY. (2002). The effect of laser treatment on skin to enhance and control transdermal delivery of 5-fluorouracil. J Pharm Sci, 91:1613–1626.
5. Becker SM, Kuznetsov AV. (2008). Thermal in vivo skin electroporation pore development and charged macromolecule transdermal delivery: A numerical study of the influence of chemically enhanced lower lipid phase transition temperatures. Int J Heat Mass Transf, 51:2060–2074.
6. Kaushik S, Hord AH, Denson DD, McAllister DV, Smitra S, Allen MG et al. (2001). Lack of pain associated with microfabricated microneedles. Anesth Analg, 92:502–504.
7. Ito Y, Hagiwara E, Saeki A, Sugioka N, Takada K. (2006). Feasibility of microneedles for percutaneous absorption of insulin. Eur J Pharm Sci, 29:82–88.
8. Henry S, McAllister DV, Allen MG, Prausnitz MR. (1998). Microfabricated microneedles: a novel approach to transdermal drug delivery. J Pharm Sci, 87:922–925.
9. Wei-Ze L, Mei-Rong H, Jian-Ping Z, Yong-Qiang Z, Bao-Hua H, Ting L, et al. (2010). Super-short solid silicon microneedles for transdermal drug delivery applications. Int J Pharm, 389:122–129.
10. Gill HS, Prausnitz MR. (2008). Pocketed Microneedles for Drug Delivery to the Skin. J Phys Chem Solids, 69:1537–1541.
11. Martanto W, Davis SP, Holiday NR, Wang J, Gill HS, Prausnitz MR. (2004). Transdermal delivery of insulin using microneedles in vivo. Pharm Res, 21:947–952.
12. Gill HS, Prausnitz MR. (2007). Coated microneedles for transdermal delivery. J Control Release, 117:227–237.
13. Kolli CS, Xiao J, Parsons DL, Babu RJ. (2012). Microneedle assisted iontophoretic transdermal delivery of prochlorperazine edisylate. Drug Dev Ind Pharm, 38:571–576.
14. Wong LW, Sun WQ, Chan NW, Lai WY, Leung WK, Tsang JC, et al. (2007). Zeolite microneedles for transdermal drug delivery. Stud Surf Sci Catal, 170 (A): 525–530.
15. Sullivan SP, Murthy N, Prausnitz MR. (2008). Minimally invasive protein delivery with rapidly dissolving polymer microneedles. Adv Mater, 20:933–938.
16. Lee JW, Park JH, Prausnitz MR. (2008). Dissolving microneedles for transdermal drug delivery. Biomaterials, 29:2113–2124.
17. Ito Y, Murakami A, Maeda T, Sugioka N, Takada K. (2008). Evaluation of self-dissolving needles containing low molecular weight heparin (LMWH) in rats. Int J Pharm, 349:124–129.
18. Miyano T, Tobinaga Y, Kanno T, Matsuzaki Y, Takeda H, Wakui M et al. (2005). Sugar micro needles as transdermic drug delivery system. Biomed Microdevices, 7:185–188.
19. Donnelly RF, Raj Singh TR, Woolfson AD. (2010). Microneedle-based drug delivery systems: microfabrication, drug delivery, and safety. Drug Deliv, 17:187–207.
20. Ito Y, Kashiwara S, Fukushima K, Takada K. (2011). Two-layered dissolving microneedles for percutaneous delivery of sumatriptan in rats. Drug Dev Ind Pharm, 37:1387–1393.
21. Park JH, Allen MG, Prausnitz MR. (2006). Polymer microneedles for controlled-release drug delivery. Pharm Res, 23:1008–1019.
22. Li G, Badkar A, Nema S, Kolli CS, Banga AK. (2009). *In vitro* transdermal delivery of therapeutic antibodies using maltose microneedles. Int J Pharm, 368:109–115.
23. Miyano T, Miyachi T, Okanishi T, Todo H, Sugibayashi K, Uemura T, et al. (2007). Hydrolytic microneedles as transdermal drug delivery system. Transducers, 1:355–8, Proceedings of the 14th International Conference on Solid-State Sensors, Actuators and Microsystems, Lyon, France, June 10–14.
24. Donnelly RF, Morrow DI, Singh TR, Migalska K, McCarron PA, O'Mahony C et al. (2009). Processing difficulties and instability of carbohydrate microneedle arrays. Drug Dev Ind Pharm, 35:1242–1254.
25. Park JH, Choi SO, Seo S, Choy YB, Prausnitz MR. (2010). A microneedle roller for transdermal drug delivery. Eur J Pharm Biopharm, 76:282–289.
26. Ito Y, Yoshimitsu J, Shiroyama K, Sugioka N, Takada K. (2006). Self-dissolving microneedles for the percutaneous absorption of EPO in mice. J Drug Target, 14:255–261.
27. Ito Y, Ise A, Sugioka N, Takada K. (2010). Molecular weight dependence on bioavailability of FITC-dextran after administration of self-dissolving micropile to rat skin. Drug Dev Ind Pharm, 36:845–851.
28. Sun G, Chu C-C. (2006). Synthesis, characterization of biodegradable dextran-allyl isocyanate-ethylamine/polyethylene glycol-diacrylate hydrogels and their in vitro release of albumin. Carbohydr Polym, 65:273–287.
29. Pasut G, Veronese FM. (2007). Polymer-drug conjugation, recent achievements and general strategies. Prog Polym Sci, 32:933–961.
30. Mellott MB, Searcy K, Pishko MV. (2001). Release of protein from highly cross-linked hydrogels of poly(ethylene glycol) diacrylate fabricated by UV polymerization. Biomaterials, 22:929–941.
31. Sullivan SP, Koutsonanos DG, Del Pilar Martin M, Lee JW, Zarnitsyn V, Choi SO et al. (2010). Dissolving polymer microneedle patches for influenza vaccination. Nat Med, 16:915–920.
32. Chan V, Zorlutuna P, Jeong JH, Kong H, Bashir R. (2010). Three-dimensional photopatterning of hydrogels using stereolithography for long-term cell encapsulation. Lab Chip, 10: 2062–2070.
33. Kang L, Hancock MJ, Brigham MD, Khademhosseini A. (2010). Cell confinement in patterned nanoliter droplets in a microwell array by wiping. J Biomed Mater Res A, 93:547–557.
34. Khademhosseini A, Yeh J, Jon S, Eng G, Suh KY, Burdick JA et al. (2004). Molded polyethylene glycol microstructures for capturing cells within microfluidic channels. Lab Chip, 4: 425–430.
35. Phillips AJ. (2007). Contact Lenses. London: Elsevier:548–549.
36. Kazmierska KA, Ciach T. (2009). Bioactive coatings for minimally invasive medical devices: Surface modification in the service of medicine. Recent Pat Biomed Eng, 2:1–14.
37. Ahn D, Jeong YC, Lee S, Lee J, Heo Y, Park JK. (2009). Control of liquid crystal pretilt angles by using organic/inorganic hybrid interpenetrating networks. Opt Express, 17: 16603–16612.
38. Varshney M, Khanna T, Changez M. (1999). Effects of AOT micellar systems on the transdermal permeation of glyceryl trinitrate. Colloids Surf B Biointerfaces, 13:1–11.
39. Park JH, Allen MG, Prausnitz MR. (2005). Biodegradable polymer microneedles: fabrication, mechanics and transdermal drug delivery. J Control Release, 104:51–66.

40. Kerwin BA, Remmele RL Jr. (2007). Protect from light: photodegradation and protein biologics. J Pharm Sci, 96:1468–1479.
41. Kindernay J, Blažková A, Rudá J, Jančovičová V, Jakubíková Z. (2002). Effect of UV light source intensity and spectral distribution on the photopolymerisation reactions of a multifunctional acrylated monomer. J Photochem Photobiol A Chem, 151:229–236.
42. Donnelly RF, Singh TR, Tunney MM, Morrow DI, McCarron PA, O'Mahony C et al. (2009). Microneedle arrays allow lower microbial penetration than hypodermic needles in vitro. Pharm Res, 26:2513–2522.
43. Xie Y, Xu B, Gao Y. (2005). Controlled transdermal delivery of model drug compounds by MEMS microneedle array. Nanomedicine, 1:184–190.
44. Brown MB, Traynor MJ, Martin GP, Akomeah FK. (2003). Transdermal drug delivery. In: Jain KK, ed. Drug Delivery Systems. Basel: CRC Press:119–139.